

THEORETICAL STUDIES OF A PULSED PLASMA MICROTHRUSTER

P.G. Mikellides, P.J. Turchi,
R.J. Leiweke, C.S. Schmahl, I.G. Mikellides
The Ohio State University
Columbus, OH

ABSTRACT

Numerical simulations, using the MACH2 code, have been carried out for a Teflon-fed, benchmark PPT system. The computations are performed in the plane of the current flow and include the same non-monotonic heat flux algorithm that was successfully implemented in the findings of late-time ablation during simulations of the LES-6 thruster. Present results indicate proper capturing of the benchmark thruster's overall electromagnetic behavior, along with the linear trends of ablated mass and impulse-bit with respect to input energy. A substantial discrepancy between mass loss during the pulse and total ablated mass is again found, suggesting the potential for considerable performance improvement. Late-time calculations show that this mass loss is dependent on moderate, elevated Teflon for the initial temperature. A simple diffusion calculation based on the repetitive nature of the heat pulses suggests a simple direction for improving performance.

INTRODUCTION

The pulsed plasma thruster's (PPT) tested ability (for over two-decades) to provide small impulse bits and high specific impulse at low power levels (30-500 W), establishes it as a favored propulsion system, especially for station-keeping missions.^{1,2,3} The thruster's operational simplicity and robustness, allowed for extensive empirical analysis, mainly during the 1960's and 70's. A renewed interest for the aforementioned small satellite missions, including the possibility of orbit-raising and maneuvering, has initiated further investigation, aiming toward improvement of the overall low thrust efficiencies, observed in laboratories.

The basic operation of the PPT consists of repeated discharge pulses across a Teflon surface. Useful thrust is mainly produced by the electromagnetic acceleration of the ablated mass that

has been ionized. The main scientific deficiency is the lack of full understanding of the process of ablating mass from solid propellants. This does not allow independent computation of either the mass-flow rate or exhaust speed which in turn precludes specific insights that would allow performance improvements. For this reason, PPTs have not yet performed at efficiencies higher than 12%.³

Recent numerical modelling⁴ of the LES-6 thruster, using the two-dimensional, magnetohydrodynamic (MHD) code, MACH2,⁵ and comparisons with experimental data, provide helpful insights in regard to mass being ablated from the propellant surface between pulses. This post-pulse mass loss at low speeds substantially diminishes the thruster's efficiency and specific impulse. Further investigation of the heat processes within the thruster is being carried out on both theoretical and experimental fronts.

The present paper discusses the most recent results from numerical simulations that have been carried out for the benchmark PPT.⁶ This system, operated at the NASA Lewis Research Center, provides easier access to thruster components, thus allowing more flexibility and better coupling between theory and experiment. It has been operated at higher energy levels than the LES-6¹ (2J vs 40J) acquiring a substantial amount of experimental data.

BACKGROUND

Previous computations⁴ with the MACH2 code of the PPT thruster utilized for the LES-6 satellite¹ have led to the following insights:

a) The calculated mass ablated, during discharge pulses of approximate duration of 3 μ sec, significantly underestimated the experimental values taken as an average over a number of pulses at 2 Hz frequency.

b) Computations during post-discharge times have shown a finite evaporation rate. Its magnitude depended on the "base" temperature chosen for the initial and constant temperature boundary. This implied that elevated Teflon temperatures due to the repetitive nature of heat application and/or heating from the surroundings could be the cause of late-time mass loss.

c) Calculated impulse bit agreed well with the experiment, however, there only two experimental points available.

d) The discrepancy between the computed ablated mass during the discharge and the total ablated mass was significant enough to degrade the thruster's performance by one order of magnitude.

The above have led to the initiation of a new research effort at The Ohio State University. Experiments with the benchmark PPT are focused in the overall thermal management of the thruster. Measurements of the Teflon temperature distribution have been carried out within the Teflon propellant and at various stations in the PPT circuit. Preliminary results⁷ have shown that the Teflon reaches temperatures in excess of 370K at a depth of 3 mm from the exposed ablating surface.

THEORETICAL MODELING

The MACH2 code is the primary tool used here, for calculating the PPT discharge flow field, including the propellant ablation process. It is a two-dimensional, MHD computational tool for problems of complex geometry in plane parallel or cylindrical symmetry. The single fluid, multi-temperature code employs an Implicit Continuous Eulerian, Arbitrary Lagrangian Eulerian (ICE-ALE) scheme and it is fully pointered for minimum code size. MACH2 incorporates a variety of models for Hall effect, viscous stress, non-equilibrium radiation, anomalous transport and electrical circuitry. It utilizes the SESAME Equation-of-State⁹ library (developed by the T-1 Division at Los Alamos National Laboratory) for thermodynamic and transport properties and it has been successfully applied to a variety of magnetohydrodynamic problems.

The new ablation algorithm, developed at The Ohio State University, for capturing the time-dependent, heat flux to the Teflon surface, is included in these simulations. The algorithm consists of a second-order accurate, 2-dimensional, diffusion-equation solver, (with the option of an adaptive grid for better gradient resolution at the ablating surface) in order to determine the vapor density and temperature at the ablating surface. These conditions are then used as boundary conditions for the advancement and evolution of the plasma by MACH2. The algorithm provides these values based on a calculation of the net heat flux to the solid, due to the presence of the local plasma and the evaporating surface. A vapor pressure formula,⁸

$$p_{\text{vap}} = p_0 \exp\left(\frac{-C_1}{T} + C_2\right) \quad (1)$$

where, for Teflon, p_0 is 1 atm, $C_1 = 20815.0731$ and $C_2 = 35.15265$, is used to evaluate the vapor density, according to the ideal gas law and the surface temperature computed from the energy equation. The resulting pressure gradient causes the evaporated mass to flow into the discharge. Time integration of thrust and mass flow rate provides values for the impulse bit and ablated mass. The former considers static, dynamic and magnetic pressure contributions.

BENCHMARK PPT SIMULATIONS

The geometric configuration of the benchmark PPT consists of two rectangular copper electrodes that are 1 inch wide. The computations presented here simulate the 1 inch long electrodes placed 1 inch apart. The LRC-circuit utilized consists of a 31.3 μF capacitor, a 93 nH external inductance and a 10 m Ω external resistance. The simulations are carried out for three energy settings: 20J, 40J and 60J.

The two-dimensional computational region extends to about four times the thruster length downstream. This exhaust region was also extended to about two times the electrode gap on each side of the thruster's exit, thus capturing plume effects and alleviating concerns with boundary conditions at the thruster's exit where thrust computations were carried out. The plasma is a single-temperature fluid, with real equations of state as prescribed by the SESAME tables.⁹ No-slip hydrodynamic and adiabatic thermal boundary conditions were imposed at the electrodes. Radiative and viscous losses were excluded, and transport coefficients were classical. The virtual-block representing the Teflon solid was 60 microns long (about 30 times pulse diffusion lengths) with constant "base" temperature boundary condition. The same "base" temperature is utilized as a uniform initial temperature. The lateral boundaries were assumed to be adiabatic.

The typical damped, oscillating LRC-current waveform is shown in Figure 1 as calculated by MACH2 and compared to the experimental values for the 40J configuration. Figure 2 compares the voltage waveforms. In both cases the relative magnitudes and characteristic times are in good agreement. A comparison of the time-integral values of the current squared, $J^2(t)$, - indicative of impulse-bit magnitudes - shows a discrepancy of 12%.

Computations are carried out well beyond pulse times to confirm the late-time ablation behavior depicted in the LES-6 simulations. Indeed, for a base temperature of 520K, i.e., the back end of the diffusion block is kept constant at this temperature value, Figure 3 shows a finite rate of evaporation. During early post-discharge times the mass-loss rate is approximately 80 $\mu\text{g/s}$ with an average of 167 $\mu\text{g/s}$ for the duration of the calculation shown in Figure 3. The value for this base temperature is much higher than experimental values for mean temperatures in the solid as mentioned above; it is presented here only for confirmation that MACH2 does indeed compute late-time ablation rates for the benchmark configuration. For a more reasonable base temperature value of 370K, the computational timesteps required to accurately capture this late-time behavior did not allow computations into the msec time regime. At early post-discharge times, however, mass rates were calculated at 43 $\mu\text{g/s}$.

Examination of the temperature distribution within the solid during post-discharge times reveals that about 3.5 microns of Teflon are in the excess of 600K. This implies that a substantial portion of the propellant (compared to about 45 \AA ablated during the pulse), is at temperatures above the usual melting point of Teflon¹⁰ and thus in liquid state. This higher density fluid has the opportunity to mix with the lower density gas based on Rayleigh-Taylor instabilities and eventually Kevin-Helmholtz instability as it acquires some speed. Calculation of the amount of liquid mass escaping from the Teflon surface is quite difficult because it depends on the spectrum of perturbations applied to the liquid surface.

Obviously, the relative behavior and magnitudes of both ablated mass and impulse-bit during pulse and post-discharge times is of great significance as they pertain to efficiency and specific impulse. Such insights can be gained by comparing experimental values to calculated values during the discharge for both performance variables. Figure 4 depicts the approximately linear increase of ablated mass with input energy, but a significant discrepancy between average-per-pulse (represented by the experiment) and discharge-time (represented by the MACH2 computations) values is evident. Similar comparisons of the impulse-bit, shown in Figure 5, imply the same trends. Based on the relative slopes these trends can be related to efficiency and specific impulse by,

$$\eta = \frac{I_E^2}{2 m_E} , \quad I_{sp} = \frac{I_E}{m_E g} \quad (2)$$

where m_E and I_E are the slopes of ablated mass and impulse-bit with respect to input circuit energy, respectively. Based on total values measured by experiment the thruster is operating at 7.7% efficiency providing a specific impulse of 1270 sec. MACH2 calculated slopes during discharge times imply an efficiency of 27% and 6375 sec specific impulse. It is apparent that elimination of late-time mass loss can provide substantial performance improvements.

Calculations of the late-time mass loss for the base temperature of 370K have shown that indeed these magnitudes (initially above 40 $\mu\text{g/s}$) can account for the discrepancy between the calculated pulse ablation and the total mass ablated from experiment. Average thrust for the 40J case during this initial post-discharge period is calculated at 78.7 μN which if assumed constant extrapolates to account for 50% of the discrepancy, (Figure 5) in the impulse-bit.

IMPROVING PERFORMANCE

The above arguments suggest that the elevated base Teflon temperatures could be part of the cause for post-discharge mass loss. Consequently, decreasing the deposition of heat into the solid could minimize the undesired, late evaporation.

The heating of the solid propellant is a combination of applying bursts of heat energy at high frequency and heat transfer from surrounding sources, such as electrodes, capacitor, etc. If we assume that the former is the dominant mode of heating (at least for the higher energy PPTs), we can approximate the heat flux at the ablating surface as the sum of instantaneous delta functions;

$$-\kappa \frac{dT}{dx} \Big|_{x=0} = q(t) = q_0 \sum_{n=1}^N \delta(t - n/f) \quad (3)$$

where N is the number of pulses and f is the frequency at which they are applied. The above expression serves as the boundary condition for the one-dimensional diffusion equation,

$$\frac{dT}{dx} = \alpha \frac{d^2T}{dx^2} \quad (4)$$

of a finite length solid of diffusivity, $\alpha = \kappa/\rho c$, thermal conductivity, κ , solid density, ρ , and specific heat, c . The benchmark thruster was operated in a low-density vacuum tank environment. The back end of the Teflon solid was simply exposed to this vacuum, as opposed to

being in contact with an aluminum plate. We could thus model the back-end boundary condition as one of free convection,

$$-\kappa \frac{dT}{dx} \Big|_{x=L} + h(T - T_\infty) = 0 \quad (5)$$

where h is a convective coefficient and T_∞ is the temperature in the vacuum tank. The solution to the one-dimensional diffusion subject to the above boundary conditions is

$$T(x,t) = T_o + \frac{2\alpha q_o}{\kappa} \sum_m \frac{(\beta_m^2 + H^2) \cos(\beta_m x)}{L(\beta_m^2 + H^2) + H} \cdot \sum_{n=1}^N \exp(-\alpha \beta_m^2 (t - n/f)) \quad (6)$$

where $T_o = T_\infty$ is the initial uniform solid temperature at 293K, $H = h/\kappa$ and β_m are the positive roots of the transcendental equation, $\beta \tan \beta L = H$. The above solution is compared to the experimental temperature measurements of the 40J case at $x=3\text{mm}$. The length of the Teflon solid was 1 inch. Theory compares well with experiment (Figure 6) suggesting that the basic mechanisms have been captured. A few degrees discrepancy at later times suggests that radiation cooling may be important at the higher temperatures.

The profiles of both experiment and theory imply that the rate of heat deposition into the solid is much higher than the rate by which heat is conducted away from the back end. As heat is continued to be applied, the temperature reaches a steady state. At these times, all the heat is conducted through the solid and away from the back end. In operational PPTs this heat will be conducted to the large aluminum plate. This suggests an avenue for diminishing the heating of the Teflon solid by reaching steady state much earlier and at lower temperatures. This can be accomplished - within the spirit of simplicity - by reducing the length of the solid propellant. Indeed, the temperature profile for a length of 3/8 in (Figure 6) reaches steady state much faster and at much lower overall temperatures. The potential gain by reducing mass loss could compensate for the length reduction. In addition, Teflon cooling could be achieved laterally.

CONCLUSIONS

Simulations of a benchmark PPT have been performed using the MHD MACH2 code. Previous insights of late-time ablation that can significantly degrade performance have been confirmed and quantified. Heating of the Teflon propellant due to the repetitive heat application and/or heat transfer from surroundings may be the cause of this late mass loss. These elevated solid temperatures can be greatly reduced by cooling the propellant more rapidly.

Future goals are mainly focused toward improving the MACH2 model. Specifically, the real equations of state are being upgraded to include thermal non-equilibrium with appropriate transport coefficients.

ACKNOWLEDGMENTS

This work was supported by the NASA Lewis Research Center, Cleveland, OH, under grant NAG3-843, and the Ohio Supercomputer Center.

REFERENCES

1. Vondra, R.J., Thomassen, K. and Solbes, A., "Analysis of Solid Teflon Pulsed Plasma Thruster," *Journal of Spacecraft and Rockets*, Vol. 7, No. 12, Dec. 1970, pp. 1402-1406.
2. Guman, W. and Palumbo, D.J., "Effects of Propellant and Electrode Geometry on Pulsed Ablative Plasma Thruster Performance," AIAA 75-409, 11th Electric Propulsion Conference, New Orleans, LA, 1975.
3. Myers, R.M., "Electromagnetic Propulsion for spacecraft," AIAA 93-1086, Aerospace Design Conference, Irvine, CA, 1993.
4. Mikellides, P.G. and Turchi, P.J., "Modeling of Late-time Ablation in Teflon Pulsed Plasma Thrusters", *Journal of Propulsion and Power*, In Review.
5. Peterkin, R.E. Jr., Giancola, A.J., Frese, M.H. and Buff, J., "MACH2: A Reference Manual - Fourth Edition," Mission Research Corporation, 1989.
6. Kamhawi, H., Turchi, P.J. and Leiweke, R.J., "Design and Operation of a Laboratory Bench-mark PPT", AIAA 96-2732, 32nd Joint Propulsion Conference, July, 1996.

7. Kamhawi, H., Personal Communication.
8. Wentink, T., Jr., "High Temperature Behavior of Teflon," AVCO-EVERETT Research Laboratory, Contract No. AF 04(647)-278, July 1959.
9. Holian, K.S., ed, "T-4 Handbook of Material Properties Data Base, Vol IC: EOS," LA-10160-MS, Los Alamos National Laboratory, November, 1984.
10. Leiweke, R.J., Turchi, P.J., Kamhawi, H., and Myers, R.M., "Experiments with Multi-material Propellants in Ablation-Fed Pulsed Plasma Thrusters," AIAA 95-2916, 31st Joint Propulsion Conference, July, 1995.

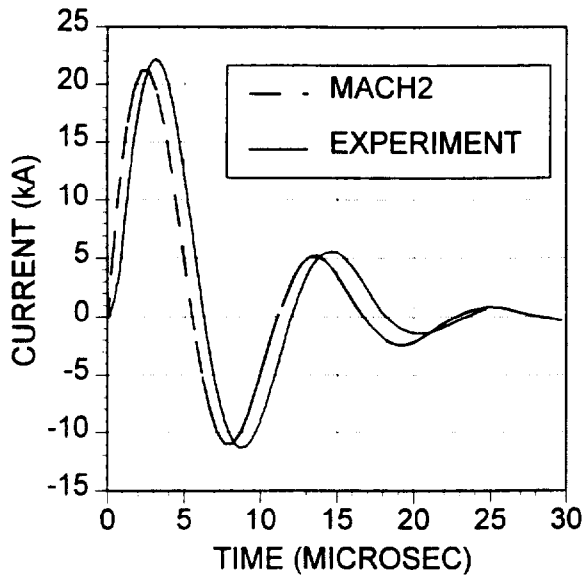


Figure 1. MACH2 calculated current waveform for the 40J case as compared to experiment.

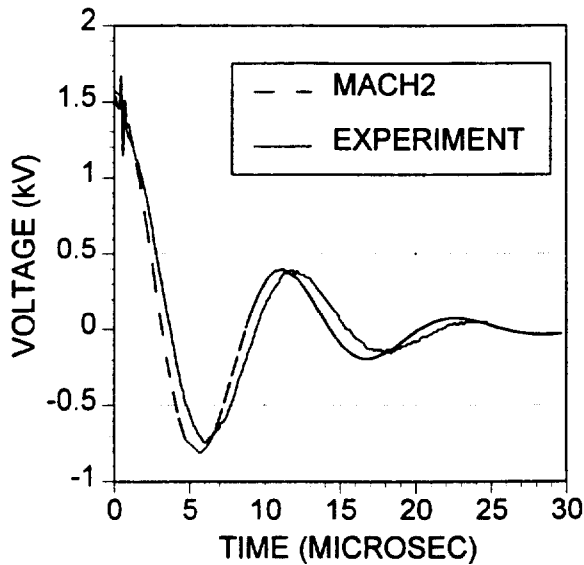


Figure 2. MACH2 calculated capacitor voltage waveform for the 40J case as compared to experiment.

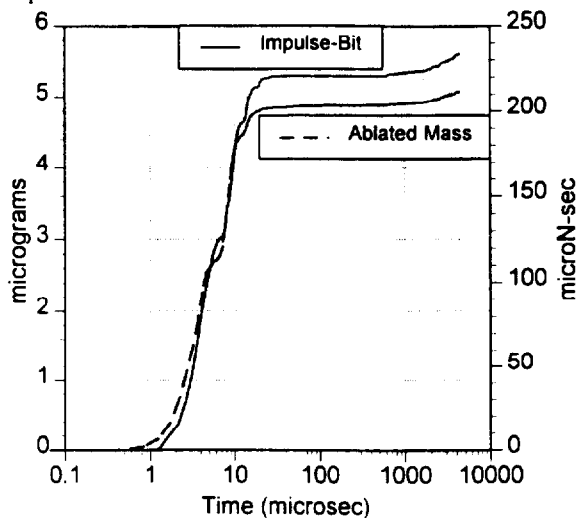


Figure 3. MACH2 mass ablated and impulse-bit histories for the 40J case.

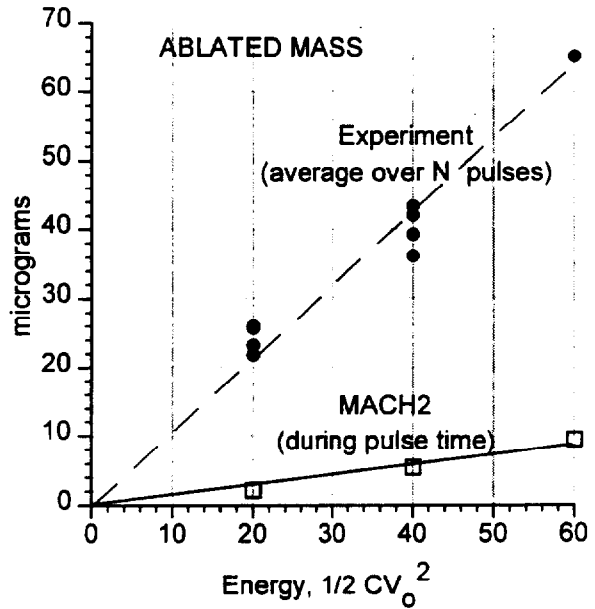


Figure 4. Calculated ablated mass during pulse as compared to total ablated mass from experiment.

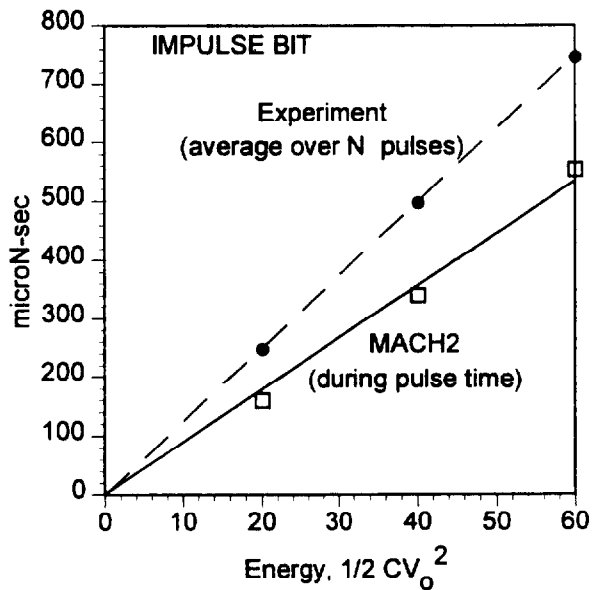


Figure 5. Calculated impulse-bit during pulse as compared to total impulse-bit from experiment.

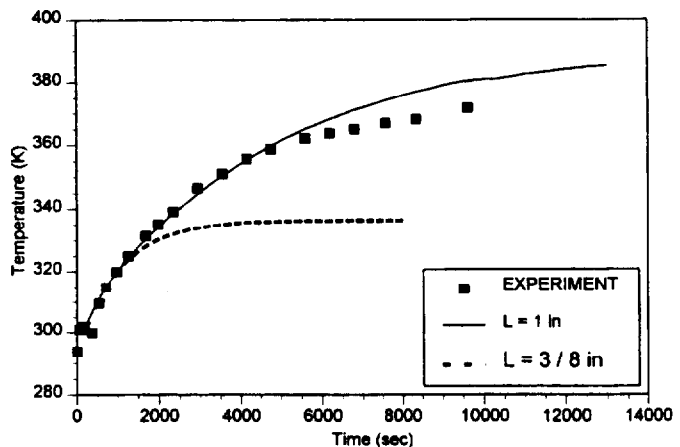


Figure 6. Teflon temperature history at 3 mm from the ablating surface for two different solid lengths.